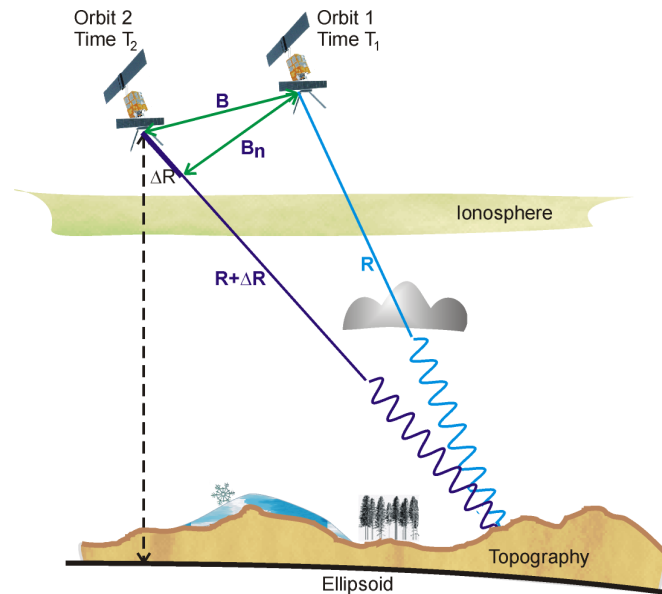


THE USE OF SYNTHETIC APERTURE RADAR (SAR) INTERFEROMETRY TO RETRIEVE BIO- AND GEO-PHYSICAL VARIABLES

FINAL REPORT – EXECUTIVE SUMMARY

EUROPEAN SPACE AGENCY STUDY CONTRACT REPORT
UNDER ESA CONTRACT NO 16366/02/NL/MM



PREPARED BY

Thomas NAGLER and Helmut ROTT
ENVEO (Prime Contractor), Exlgasse 39, A-6020 Innsbruck, AUSTRIA
<http://www.enveo.at>

Ramon HANSSEN and Dmitri MOISSEEV
Delft University of Technology, Department of Geodesy, Delft, THE NETHERLANDS

Nico ADAM, Michael EINEDER and Bert KAMPES
Remote Sensing Technology Institute, German Aerospace Center, Wessling, GERMANY

Irena HAJNSEK and Konstantinos P. PAPATHANASSIOU
Microwaves and Radar Institute, German Aerospace Center, Wessling, GERMANY

Shane R. CLOUDE
AEL-Consultants, Cupper Fife, Scotland, UNITED KINGDOM

DATE: 20 FEBRUARY 2004



The work described in this report was done under ESA contract. Responsibility for the contents resides in the author or organisation that prepared it.

ESA STUDY CONTRACT REPORT			
ESA CONTRACT NO: 16366/02/NL/MM	SUBJECT: The Use of Synthetic Aperture Radar (SAR) Interferometry to Retrieve Bio- and Geo-Physical Variables		CONTRACTOR: ENVEO
ESA CR ()No:	STAR CODE:	No of volumes: 1 This is volume no: 1	CONTRACTOR'S REF: Executive Summary of Final Report
<p>In this document an overview on the work carried out in the study is presented, examples of the main results are shown, and recommendations for further work and exploitation of study results are summarized. In the study new possibilities for retrieving bio- and geo-physical variables for land applications from interferometric SAR (InSAR) data were investigated. InSAR retrieval algorithms were developed for the following parameters: (i) atmospheric water vapour, (ii) snow water equivalent (SWE, the mass of snow on ground), and (iii) forest height.</p> <p>In Section II the information content of interferograms on physical properties of the atmosphere is discussed, methods for resolving the acquisition ambiguity (isolating the atmospheric phase term for single dates) and for coherence optimisation are presented and an example for interpretation of the atmospheric signal, based on ERS SAR repeat pass data, is shown. In Section III an algorithm for SWE retrieval from repeat pass SAR data is presented, the effects of snow cover changes on coherence are discussed, and examples of SWE retrievals are presented for ERS SAR data and for L-band airborne E-SAR data. In Section IV a method to retrieve forest height from dual-polarized single-pass interferometric data (Light-Pol InSAR) is presented, an example for forest height estimation from L-band airborne SAR in dual-pol and quad-pol configuration is shown, and possibilities and limitations of various polarisations and radar frequencies are discussed. Section V provides information on InSAR data processing issues in support of SWE and water vapour retrievals.</p>			
<p>The work described in this report was done under ESA Contract. Responsibility for the contents resides in the author or organisation that prepared it.</p>			
<p>AUTHORS: Thomas Nagler, Helmut Rott (ENVEO, Innsbruck, AT), Ramon Hanssen, Dmitri Moisseev (DEOS, Delft, NL), Irena Hajnsek, Konstantinos P. Papathanassiou (HR-DLR, Wessling, D), Shane R. Cloude (AELc, Scotland, UK), Nico Adam, Michael Eineder, Bert Kampes (IMF-DLR, Wessling, D)</p>			
ESA STUDY Manager:		ESA BUDGET HEADING	
N. Flourey (TOS-EEP)		060 - GSP	

Amendment Record:

16 February 2004	Draft Version
20 February 2004	Final Version

TABLE OF CONTENTS

I	Objectives.....	1
II	InSAR retrieval of atmospheric variables	1
II.1	Background and goals.....	1
II.2	Water vapour mapping importance.....	3
II.3	Acquisition ambiguity resolution and coherence optimisation.....	3
II.4	Decomposition and interpretation.....	5
II.5	Outlook	5
III	InSAR retrieval of snow and ice parameters	6
III.1	Introduction.....	6
III.2	The algorithm for SWE retrieval	6
III.3	Coherence of snow covered areas.....	8
III.4	Case study with ERS SAR data	9
III.5	Case study with airborne L-band SAR data.....	10
III.6	Conclusion and outlook	11
IV	InSAR retrieval of vegetation parameters.....	12
IV.1	Introduction.....	12
IV.2	Modelling and inversion algorithm.....	12
IV.3	Discussion of the results	13
IV.4	Quad-Pol and Temporal Decorrelation.....	14
V	Data processing.....	15
V.1	Snow and ice.....	15
V.2	Atmosphere.....	16
V.3	Conclusion and recommendations	17
VI	References	17

This page is intentionally left blank.

I OBJECTIVES

The aim of the study was to define new possibilities for retrieving bio- and geo-physical variables for land applications from interferometric SAR data and to develop and test prototype retrieval algorithms for these variables. The following components of the global environmental system were considered:

1. atmosphere
2. snow and ice
3. vegetation

In the beginning of the study various parameters were identified as possible candidates for development of InSAR retrieval techniques. As next step, for each of these themes one parameter was selected for detailed work, based on literature review, theory and available data sets. InSAR techniques for man-made targets were also reviewed because these techniques were required for the development of retrieval algorithms. The selected parameters were: water vapour for theme (1), Snow water equivalent for theme (2), forest height for theme (3). For each of these parameters theoretical work on radar wave propagation and interferometric signals was carried out, and prototype retrieval algorithms were developed and tested with spaceborne or airborne InSAR data sets.

II INSAR RETRIEVAL OF ATMOSPHERIC VARIABLES

(by DUT-GEO)

II.1 *Background and goals*

Of all bio- and geophysical parameters that can be estimated using repeat-pass SAR interferometry, atmospheric parameters are probably third in terms of signal strength, right after surface topography and surface deformation/movement. This is evident from the large number of studies where atmospheric ‘noise’ is reported as a nuisance signal for e.g. topography and deformation analyses, see e.g. [7].

Atmospheric signal appears in every repeat-pass interferogram, although the signal might have a different power depending on the weather situation. The spatial spectrum of the signal shows a specific scaling behaviour, consistent with Kolmogorov turbulence theory, where the signal has increased power for increasing spatial distances.

The proverb ‘*One man’s trash is another man’s treasure*’ is particularly applicable here. Since in most areas of the world topography is known with sufficient accuracy and resolution (e.g. using the Shuttle Radar Topography Mission data), and deformation of the earth’s surface is relatively rare over the spatial and temporal scales of interferograms, the atmospheric signal can be isolated and interpreted from a meteorological point of view. This application is referred to as Interferometric Radar

Meteorology ([3]). Of course, the main condition is that the data are relatively coherent, which in general implies short temporal and perpendicular baselines.

Analysis of these ‘atmospheric interferograms’ shows interesting features associated with frontal systems, local convection and precipitation, boundary layer rolls, laminar-turbulent changes. The main characteristics that make the data interesting for meteorology are (i) the fine spatial resolution (say 40x40m), (ii) the capability to obtain night time data and the transparency of clouds to radar wavelengths, (iii) the full-column integrated character of the data, and (iv) the very high precision of the relative delay measurements. Compared with regular meteorological satellite imagery, spatial resolution is one or two orders of magnitude better and relative accuracies of 0.1 kg/m² can be obtained, showing the full columnar data instead of the upper layer of the atmosphere. These conclusions have been drawn from previous studies, e.g.[3] and [2].

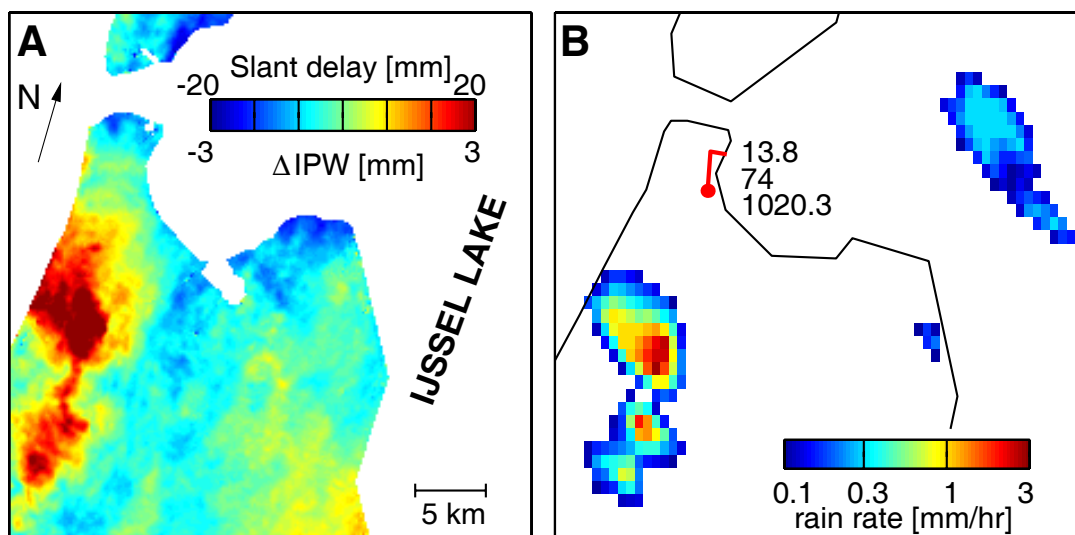


Figure II.1 Water vapour distribution associated with a precipitating cumulus cloud, in terms of delay (mm), or relative integrated precipitable water (mm or kg/m²). Left, precipitation observed by weather radar.

The main drawbacks of the technique, especially for operational meteorology and atmospheric studies are (i) the fact that interferogram data reflect the difference between two acquisitions and hence the difference between two instantaneous states of the atmosphere. This is referred to as the acquisition ambiguity. Second, (ii), the sensitivity to changing land cover on earth makes the application of the technique difficult over vegetated and humid areas and over longer time intervals. Third, (iii), the decomposition of the delay signal into meteorological parameters such as water vapour, temperature, and liquid water effects is difficult, although a likely first-order decomposition can be made. In first order, at least 90% of the observed signal is due to the water vapour distribution. Finally, (iv), the infrequent temporal sampling currently prevents real-time operational applications of the data.

In this study we aim to lift Interferometric Radar Meteorology one step closer to operationality by addressing the first three problems listed above, with main emphasis to the resolution of the acquisition ambiguity. The key concept behind this approach is to use time series of radar acquisitions, in fact, to use all available acquisitions over a specific site. Below, we will discuss the three problems addressed in this study. First, we give a short rationale behind the scientific aims.

II.2 Water vapour mapping importance

Water vapour is one of the most important variables for climate studies. At the same time, it is the parameter that is least understood. It is the principal contributor to the greenhouse effect and plays a key role in our understanding of the climate and its sensitivity to increasing levels of carbon dioxide. On small scales, less than 100 km, the moisture variability at the lower layers of the troposphere is important to know for various disciplines. For example, in regions with strong and rapidly evolving moisture gradients thunderstorms can easily develop. For non-stormy environments, 20% of the variance in the mixing ratio is found to be at scales smaller than 100 km, for stormy situations this number is 32%. Knowledge on the fine-scale distribution is also important for pin-point forecasting, hydrometeorology and studies of atmospheric radiation. The lack of knowledge of the water vapour distribution constrains the lower bound of the resolution of current Numerical Weather Models.

Current means for collecting water vapour data include radiosondes, surface-based radiometers, satellite radiometers, and GPS networks. Each of these systems has limitations, ranging from spatial sampling, spatial extent, vertical sampling, temporal sampling, data accuracy, to the cost of operation. Spaceborne Interferometric Radar Meteorology would introduce an incredibly high spatial resolution, extremely accurate delay data, against relatively low costs as a spin-off product. Of course, disadvantages are the narrow swath width, the vertically integrated character of the data, and the sparse temporal sampling. Nevertheless, it can be concluded that it is a complementary data source, revealing atmospheric processes that are impossible to observe with any other means.

These considerations justify increased attention from space agencies to facilitate suitable data acquisitions, from radar scientists and engineers to translate the data to meteorological parameters, and from the meteorological community to interpret and learn from these data.

II.3 Acquisition ambiguity resolution and coherence optimisation

The refractivity distribution at the time of an (instantaneous) radar acquisition will produce an inhomogeneous delay distribution over the SAR image, the atmospheric phase screen (APS). Since the delay observations are all relative, the signal is restricted to differences between pixels. This could be referred to as the first difference. As it is impossible to distinguish the geometric or delay contribution from the scattering contribution of the phase value, it is necessary to form interferometric differences between SAR images, the interferograms. Hence, in total the interferometric observations can be regarded as double-difference observations. The refractivity distribution at time t_1 is subtracted from the distribution at t_2 . Of course,

the differential refractivity is ambiguous, which makes it difficult to interpret the data. Usually, the nature and shape of isolated anomalies enables a reasonable guess on its origin, but this is far from robust. Unfortunately, direct resolution of the acquisition ambiguity is not possible due to the inherent rank deficiency. Nevertheless, we present two approaches to obtain reasonable estimates of the single acquisition phase screen. The first is a single-master stack, where one master image is interfered with many slave images. This approach leads to a reasonable estimate of the master image APS. Consequently, the slave APS's can be estimated. The single-master stack can be applied in two settings: conventional interferograms and Permanent Scatterers. For conventional interferograms, it is shown that the restrictions to baseline length and temporal decorrelation are generally very strict, which makes this approach only applicable in special cases. Permanent Scatterer (PS) analysis allows for the estimation of the APS per PS per image. Unfortunately it is very difficult to assess the quality of this estimation, since the size of the areas for which PS analyses are performed are generally not full-image. Stochastic validation, based on the expected Kolmogorov turbulence characteristics is performed, but proved to be very sensitive to the point noise per PS per acquisition, disturbing the power spectra used in the evaluation. Moreover, the PS analysis requires a separation of long wavelength APS signal and point noise, which can be implemented using a filter. The characteristics of this filter are only superficially known in general, resulting in difficulties in assigning the APS contribution.

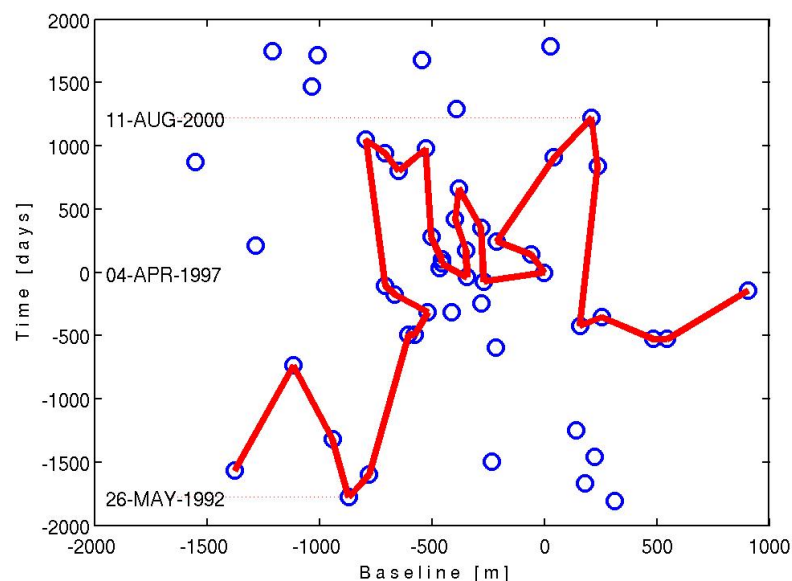


Figure II.2 Cascade of interferograms used for estimating atmospheric phase screen. Path selected using simulated annealing algorithm.

The second approach is the cascade, in which interferograms are computed where each contributing acquisition is used one time as slave and one time as master. The optimal combination of acquisitions is chosen based on the characteristics of the

perpendicular and temporal baselines. This way, for arid areas a different choice can be made than for humid areas. From the analysis it can be concluded that it is possible to resolve the acquisition ambiguity in a satisfying matter, producing single-acquisition APS estimates that can be used for interpretation. The main requirement of the method is to use as many combinations as possible, preferably all acquisitions with the same track and frame number.

II.4 Decomposition and interpretation

In this study specific attention was paid to the contribution of liquid water (rain, clouds) to the observed phase delay. Based on theoretical considerations it was concluded that liquid water may cause an additional phase delay for C-band radar of up to a few millimetres. In general, the estimate of the liquid-induced delay were in the order of 3% of the total wet delay or less. The interpretation of the estimated APS per acquisition in the Las Vegas case study showed interesting phenomena, related to orographic lifting and blocking, convection, and rolls. Particularly, the Las Vegas Convergence Zone (LVCZ), an atmospheric phenomenon specific for the Las Vegas area was interesting to evaluate using these data. Clear-air water vapour effects, in the absence of clouds, give a new perspective to the atmospheric dynamics of the region.

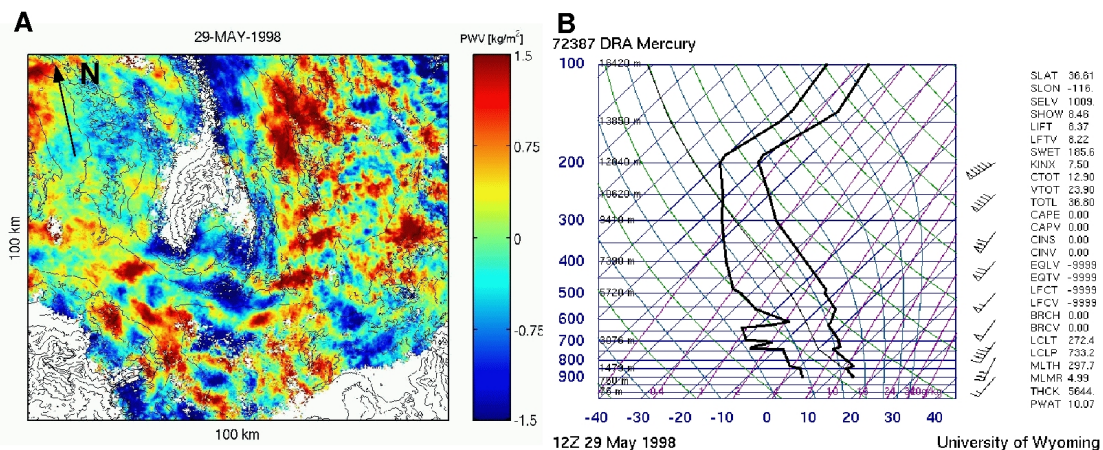


Figure II.3 Estimated water vapour field from ERS SAR data for 29 May 1998 (A) and (B) the corresponding sounding (test area Las Vegas).

II.5 Outlook

Resolving the acquisition ambiguity and identifying the contributing parameters in the atmospheric phase screen are the major achievements of this study. As such, the methodology of Interferometric Radar Meteorology reaches a new phase, making it easier for meteorologists to interpret the water vapour maps. In particular, the fact that *all* radar acquisitions can be analysed for their atmospheric signal makes both the archived and future data of SAR satellites extremely valuable. Nevertheless, it is necessary to convince the meteorological community from the benefits and potential of the technique, and to stimulate atmospheric studies in this field. Therefore, it is recommended to perform a full-scale and in-depth meteorological analysis of, say, 20

areas of interest in different climatological settings using the cascade technique. For example, using the severe weather databanks it would be valuable to search for specific atmospheric circumstances where fine-resolution, high-accuracy data are usually lacking. Producing such a large set of examples is expected to be the best way to foster research in InSAR techniques for atmospheric science.

Further recommendations can be made to the development of L-band sensors, which combine less sensitivity to temporal decorrelation with a relaxed constraint on the maximum baseline length. This would lead to a larger percentage of meteorologically interpretable data. The combination of such an L-band sensor with ScanSAR technology and a high orbital repeat frequency would lead to an optimal coverage of the world and wider, hence better interpretable, swaths. The slight reduction in spatial resolution is acceptable for such configurations.

III INSAR RETRIEVAL OF SNOW AND ICE PARAMETERS

(by ENVEO)

III.1 Introduction

Based on literature review and theory, in the initial phase of the project the following three snow and ice parameters were identified as promising candidates for the development of new retrieval techniques based on radar interferometry:

- (1) Diagenetic glacier facies (related to SAR penetration depth),
- (2) extent of melting snow areas,
- (3) snow water equivalent (SWE).

Because of the urgent need for spatially distributed SWE data for hydrology, water management and climate research and the high innovative potential, SWE was finally selected for algorithm development. Up to now no method exists which enables reliable mapping of SWE in complex terrain. Retrieving SWE from SAR backscattering data, for example, suffers from the insensitivity of long wavelengths (L- and C-band) to dry winter snow, whereas at short wavelength the snow metamorphic state becomes important.

III.2 The algorithm for SWE retrieval

The mass of snow on ground, the snow water equivalent (SWE) is the amount of water that would be obtained if a snowpack is completely melted. It may be specified as equivalent depth of water [mm] or as mass deposited on a unit surface area [kg/m^2]: $SWE = \langle \rho_s \rangle \cdot d_s$, where ρ_s is snow density and d_s is the depth of the snow pack; $\langle \cdot \rangle$ denotes the mean value over the snow pack. For dry snow a nearly linear relation exists between density and the real part of the complex permittivity [4]:

$$\varepsilon'_s = 1 + 1.60\rho_s + 1.86\rho_s^3 \quad (\text{III.1})$$

where ρ_s is specified in $[\text{g}/\text{cm}^3]$. The dielectric losses of dry snow are small, resulting in a typical penetration depth of about 20 m at C-band, whereas for wet snow it is of the order of few centimetres only. Theoretical backscatter modelling was carried out at C- and L-band for various snow and soil conditions to assess the various signal contributions and their dependence on physical properties of the targets.

The selected InSAR SWE retrieval algorithm, first proposed by Guneriusen *et al.* [1], exploits the large penetration depth in dry snow. As known from modelling and experimental data, the main contribution of backscattering from ground covered by dry winter snow stems from the ground surface. Neglecting volume scattering in the snow pack, which is very small at C-band and lower frequencies, the interferometric phase shift in snow, ϕ_{snow} , can be interpreted in terms of SWE. Figure III.1 illustrates the difference of the geometric path of the radar beam in air versus the path with a snow layer present: $\Delta R = \Delta R_s - (\Delta R_a + \Delta R_r)$.

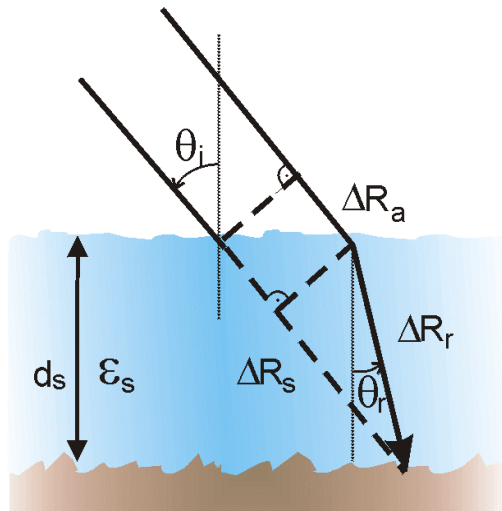


Figure III.1: Propagation path of radar wave in snow.

For calculating the phase shift in snow, the different propagation constants between air and snow have also to be taken into account. A uniform snow layer with the depth d_s , accumulating in the time between the acquisition of the two SAR images of an interferogram, causes the following phase shift [1]:

$$\phi_{snow} = -\frac{4\pi}{\lambda_i} d_s \left(\cos \theta_i - \sqrt{\epsilon'_s - \sin^2 \theta_i} \right) \quad (\text{III.2})$$

With the relation between snow density and permittivity ϵ' (Equ. III.1), the dependence of the interferometric phase on SWE can be approximated by a linear relation for $\rho_s \leq 500 \text{ kg}/\text{m}^3$. For an incidence angle $\theta_i = 23^\circ$ the phase shift due to a change of SWE is given by [1]

$$\Delta \phi_{snow} = -\frac{4\pi}{\lambda_i} 0.87 \Delta SWE \quad (\text{III.3})$$

which means that at the ERS wavelength one fringe is equivalent to 32.5 mm SWE, and for L-band ($\lambda = 24$ cm, $\theta_i = 23^\circ$) one fringe corresponds to SWE = 138 mm. In order to derive ϕ_{snow} from repeat pass SAR data, it is necessary to separate it from the other phase terms by means of differential processing. The repeat-pass interferometric phase ϕ of a non-moving pixel consists of the following contributions:

$$\phi = \phi_{flat} + \phi_{topo} + \phi_{atm} + \phi_{snow} + \phi_{noise} \quad (III.4)$$

where ϕ_{flat} and ϕ_{topo} are the phase differences due to changes of the distance satellite-target for flat earth and for topography, respectively, and ϕ_{atm} results from changes in atmospheric propagation.

III.3 Coherence of snow covered areas

A precondition for the application of InSAR is coherence of the radar signal over the interferometric time span. Theory and analysis of InSAR data sets revealed that effects of (1) surface melt, (2) snow fall, or (3) snow drift (wind erosion and deposition) are the main factors for temporal decorrelation of SAR data of snow covered areas. Because the SWE retrieval is carried out for dry snow, the first factor is of no relevance. The other two factors result in changes of the structure and roughness of the snow-surface at sub-pixel scale, changing the radar propagation path in the snow pack from each surface element. For estimating these effects, we derived an expression for temporal decorrelation of ground covered by dry snow, following the formulation developed by Zebker and Villasenor [6] for volume scattering media. Assuming that the roughness of the ground and snow surfaces are different, the following expression for temporal decorrelation of snow covered ground was derived:

$$|\gamma_{temporal}| = \exp \left[-\frac{1}{2} \left(\frac{4\pi}{\lambda_0} \right)^2 \sigma_z^2 \left(\cos \theta_i - \sqrt{\varepsilon - \sin^2 \theta_i} \right)^2 \right] \quad (III.5)$$

where σ_z is the standard deviation of the geometric path length through the snowpack at vertical. In this model the phase delay in snow is described by a Gaussian probability distribution. With this equation the decorrelation for C-band (5.3 GHz) and L-band (1.2 GHz) was calculated in dependence of surface roughness, assuming a rough ground surface and a perfectly flat snow surface (Figure III.2).

The model calculations in Figure III.2 are shown for three different snow densities, where 100 kg/m^3 is the typical density of fresh snow falling without much wind, whereas 300 kg/m^3 is the mean density of dry winter snow in the Alps. Surfaces in mountainous terrain, which are a prime target for SWE retrieval, are often characterized by surface roughness and undulations over a wide range of scales. At ERS SAR pixel scale ground surface roughness variability is of the order several centimetres, whereas the snow surfaces are usually much smoother, resulting in small-scale changes of ϕ_{snow} . The model calculations indicate that decorrelation due to snow fall and snow drift is a major problem at C-band, as confirmed by the analysis of ERS InSAR data. At L-band much better temporal phase stability can be expected.

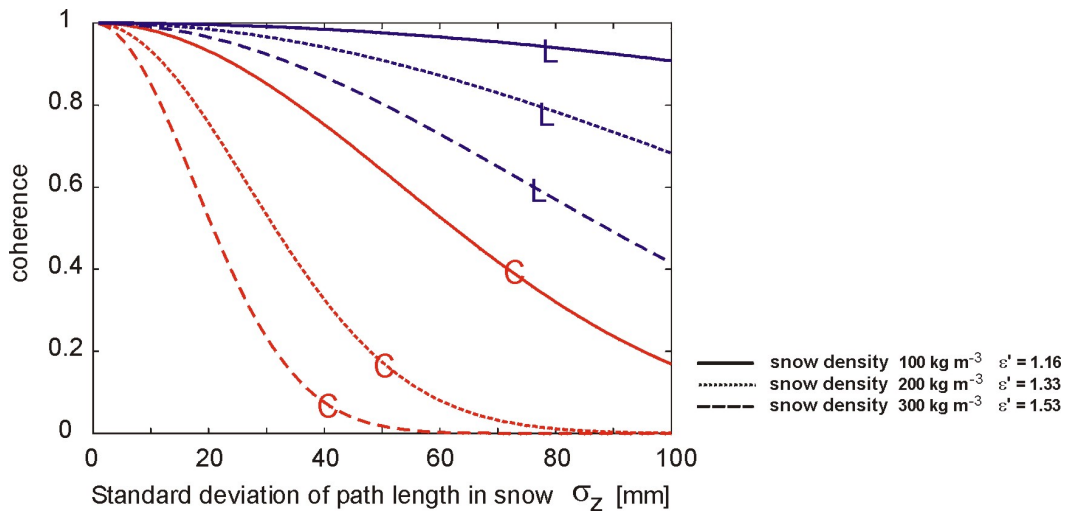


Figure III.2: Model calculations of decorrelation due to path length variations in snow at C- and L-band.

III.4 Case study with ERS SAR data

To derive SWE from an interferogram, ϕ_{snow} has to be separated from the other phase contributions shown in Equ. III.4. The topographic phase can either be calculated using a very accurate DEM and precision orbit data or using one or several interferograms under stable conditions. We used one-day or three-day ERS repeat pass data from winter without snowfall or from the summer season to retrieve ϕ_{topo} , and applied differential processing to separate ϕ_{snow} and ϕ_{topo} . Because it is not possible to separate the atmospheric phase term, ϕ_{atm} , we estimated possible errors for SWE retrievals introduced by neglecting the differences of ϕ_{atm} in the two SAR images. Model calculations, using radiosonde measurements from Austrian stations, showed that the typical winter case for dry snow conditions would introduce an atmospheric phase delay $\delta\phi_{atm} \cong 0.2 \text{ rad}$ over an altitude range of 1000 m, corresponding to $\Delta SWE = 1 \text{ mm}$. Even a five-fold increase of this error would be of little relevance for snow hydrology applications.

An ERS 3-day repeat pass time series of the Austrian Alps (Styria, Upper Austria) from winter 1994 was used for InSAR SWE retrieval studies. Two repeat pass pairs, which covered periods of substantial snow fall, were identified as candidates for SWE retrieval. In both cases large parts of the images decorrelated, as to be expected from the analysis of coherence effects of snow fall. Only unforested surfaces in valleys were sufficiently coherent to enable differential interferometric analysis. Fig. 3 shows an example of such an analysis for the Zeltweg area (Styria).

In the 6-day repeat pass interferogram 25 to 31 January 1994 (Figure III.3a) fringes are evident at the bottom of the valleys, whereas the forested mountain slopes are incoherent. After subtracting the topographic phase, calculated from the 3-day repeat pass interferogram of 15-18 February 1994 without snowfall, the SWE map is calculated from ϕ_{snow} according to Equ. III.3 (Figure III.3b). The analysis reveals an altitude increase of SWE from close to zero in the city of Zeltweg to about 10 mm in the surroundings and about 20 mm on the slopes above 850 m. The precipitation

measurements of the three stations (Zeltweg 3 mm, Seckau 10 mm, Oberzeiring 22 mm), confirm qualitatively the altitude gradient of SWE.

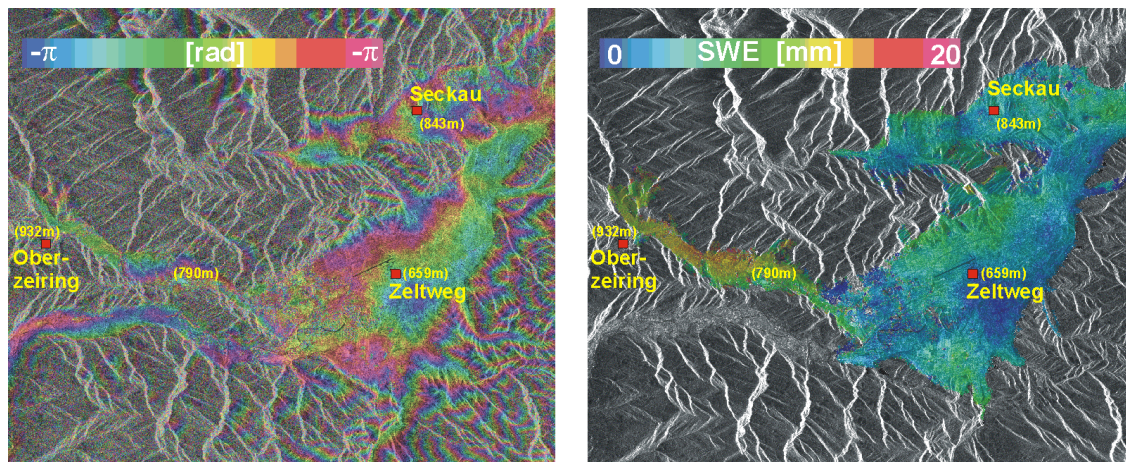


Figure III.3: ERS InSAR analysis for the Zeltweg region, Styria. (a) repeat pass interferogram 25 to 31 Jan. 1994, superimposed to an amplitude image. (b) Map of SWE (colour coded) obtained by differential processing. Areas with low coherence are in grey (image amplitude).

III.5 Case study with airborne L-band SAR data

Repeat pass airborne SAR data acquired by E-SAR of DLR at the campus in Oberpfaffenhofen [5] enabled the study of interferometric phase shifts in a snow pack. The three repeat pass scenes used for this analysis were acquired at L-band, polarimetric mode, with pulse bandwidth 100 MHz on two dates: two repeat passes within half an hour on 22 October 2002 when the site was snow free, and a third pass on 20 February 2003 when the ground was covered by dry snow. In two sub-areas 9 corner reflectors are mounted permanently. The snow inside of the trihedral reflectors had been removed before the image acquisition. In spite of snow cover in the second image, the coherence over the 4-month time span was sufficient for interferometric analysis.

Figure III.4b and III.4c show phase shifts of the corner reflectors, buildings and roads relative to the snow covered meadows. The average phase shift of the 9 corner reflectors amounted to 2.3 rad, with a standard deviation of 0.4 rad. The mean HH and VV polarized phase shifts differed only by 2 %. According to Equ. 3 a phase shift of 2.3 rad corresponds to $SWE = 43 \text{ mm}$. For snow densities of 300 kg/m^3 , 250 kg/m^3 , and 200 kg/m^3 this corresponds to snow depths of 14 cm, 17 cm, and 21 cm, respectively. No snow measurements were made at the site, but are available from Munich (snow depth 12 cm) 25 km to the east and Landsberg (20 cm) 20 km to the west. Typical densities of metamorphic winter snow are in the range of 250 to 300 kg/m^3 , which supports the conclusion that the observed phase shift is a measure of the accumulated snow.

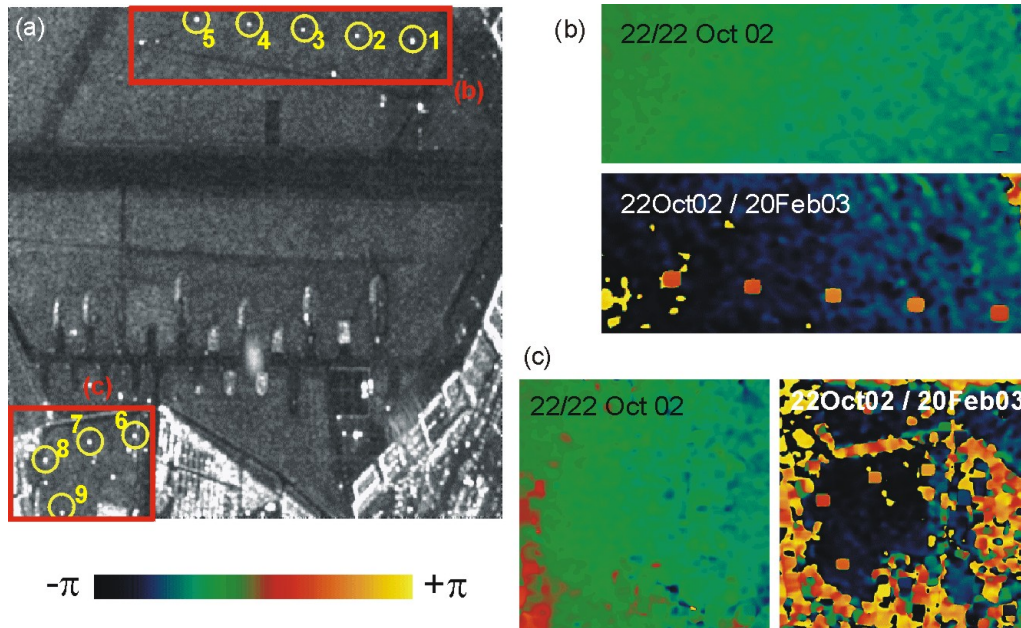


Figure III.4: (a) E-SAR L-band amplitude image of the airport at Oberpfaffenhofen with corner reflectors (yellow circles). (b) and (c) detailed view of the interferograms, VV polarisation for 22/22 October 2002 and 22 October 2002/20 February 2003, with colour coded phase.

III.6 Conclusion and outlook

The analysis of InSAR data sets and theory confirm that the interferometric phase shift of repeat pass SAR data in a dry snowpack provides a physically based means for mapping the spatial distribution of the mass of snow on ground (the snow water equivalent, SWE). The main limitations for application of this method result from temporal decorrelation due to differential phase delays at sub-pixel scale caused by snow fall or wind re-distribution. In C-band SAR data these effects often cause complete decorrelation within time spans of a few days, whereas L-band is much less affected by temporal decorrelation. Because of better coherence and larger measurement range L-band is preferable for interferometric SWE mapping compared to shorter wavelengths.

Because of the high spatial variability of snow depth and water equivalent the standard snow measurement network is too coarse for full assessment of the applicability and accuracy of the InSAR snow algorithm. For this reason it is strongly recommended to carry out dedicated experiments with airborne and spaceborne SAR during which snow measurements are carried out with great spatial detail over selected tests areas. If the InSAR SWE mapping algorithm, based on L-band repeat-pass SAR, comes up to the expectations, this would result in a major break-through for snow hydrology, water management and cryospheric research, because SWE is a very important but poorly known parameter for these applications.

IV INSAR RETRIEVAL OF VEGETATION PARAMETERS

(by DLR-HR)

IV.1 Introduction

The main objective of the Pol-InSAR Parameter Retrieval activities in this study was the investigation of the effect of a reduced observation vector and the evaluation of the impact of an available DEM on the performance of soil and vegetation parameter estimation. Based on an extensive literature review focused on quantitative soil and vegetation parameter estimation from multi-parameter InSAR observations, a list of potential soil and vegetation parameters - together with related inversion methodology and required configuration of the observation vector - has been proposed. From this list, and in agreement with ESA, forest height estimation in terms of a Dual-polarimetric (Light-Pol) single-pass interferometric (Light-Pol InSAR) configuration has been selected as the main topic for the following study.

IV.2 Modelling and inversion algorithm

One of the most successful inversion models, used widely for multi-parameter InSAR data inversion, is the Random-Volume-over-Ground (*RvOG*) model. Accordingly, forest is modelled as a single canopy layer containing randomly oriented scatterers (see Figure IV.1) located over an impenetrable ground.

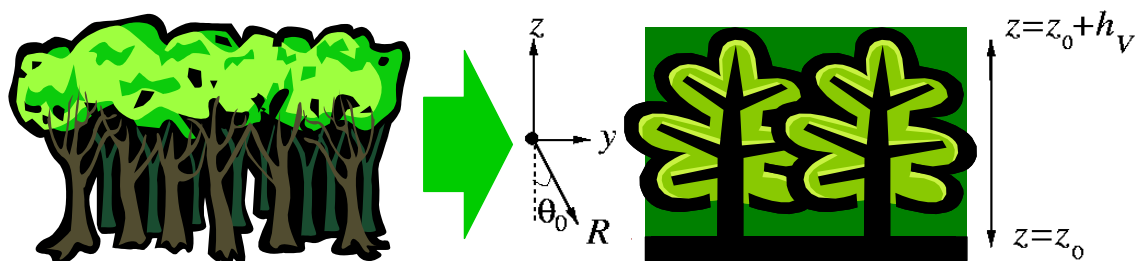


Figure IV.1: Random Volume over Ground Scattering Model.

In this case, the polarimetric/interferometric forest scattering problem in terms of four parameters: the volume thickness, the extinction coefficient of the volume that is assumed to be the same for all polarisations, the effective ground-to-volume amplitude ratio m which is the only parameter that changes with polarisation, and finally, the phase related to the underlying topography.

In a first step, the validation of the *RvOG* model has been addressed: The analysis of simulated Pol-InSAR forest data - obtained from a validated (in terms of Pol-InSAR) direct scattering model developed by Marc Williams from DSTO/Australia allowed an evaluation of the underlying scattering interdependencies and the critical assessment of the underlying assumptions made by the *RvOG* inversion model.

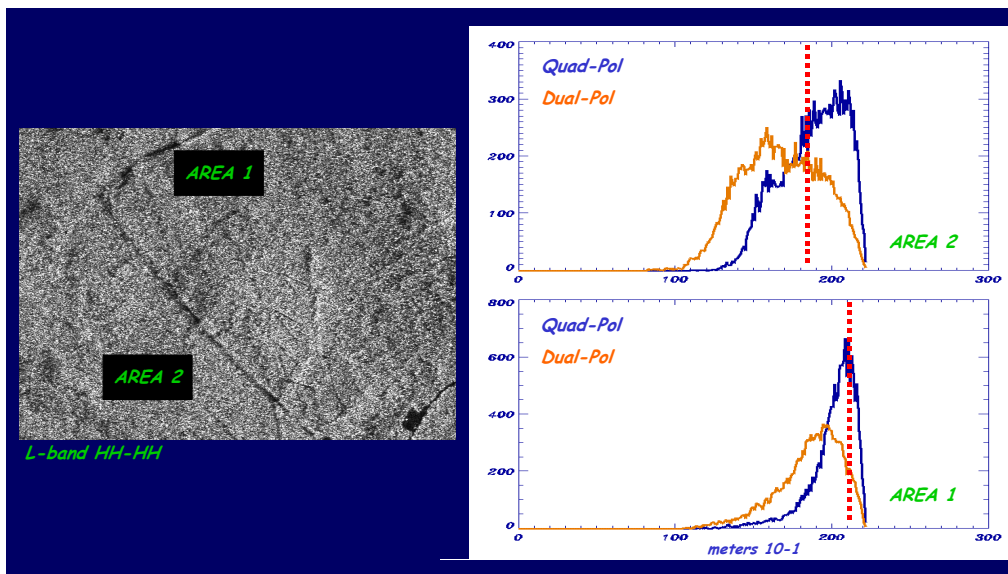


Figure IV.2: Histograms of estimated forest height for two test areas in the Fichtelgebirge/Germany test site Orange: Light-Pol InSAR, Blue: Quad-Pol InSAR, Red dots: Mean of ground measurements.

In a second step - and based on the analysis of forest simulations and experimental data sets - a modified (with respect to the Quad-Pol InSAR scenario) inversion of the *RVoG* model methodology has been developed for the inversion of forest height from Light-Pol InSAR data. Finally, in a third step, the proposed methodology has been applied on simulated as well as on experimental data sets and the obtained forest height estimated have been validated against ground measurements. The height estimates - in both cases - show an overall estimation accuracy of about 15-20% (Figure IV.2) and are sensible enough to make an impact on forest applications.

IV.3 Discussion of the results

Even if the obtained results have been encouraging, the estimation performance depends critically on a series of parameters. The first key point towards accurate forest height estimation is the precise estimation (or knowledge) of the phase related to the underlying topography. In the Dual-Pol InSAR case, model-based estimation of the underlying topography from the data is by far not so successful as in the Quad-Pol InSAR case and becomes - with decreasing overall coherence values - less robust and less accurate. It follows that, external ground elevation models - when available - may increase significantly the estimation accuracy of forest height by providing accurate information about underlying topography and its variation. However, DEM's obtained from InSAR techniques are of limited suitability for providing the required underlying topography information. The inherent vegetation bias can reach up about 80% of the forest height - depending on the operation frequency and the forest structure - making the estimation of ground topography very inaccurate. The required accuracy of a true ground topography DEM, as well as the quantification of the error introduced by a certain terrain variation have to be answered in future investigations.

A second aspect that influences directly the estimation performance of forest height is the presence of orientation effects within the forest canopy. Oriented canopy structure can lead to a polarisation dependent wave propagation through the vegetation volume and violates the assumptions of the *RVoG* model. The relevance of orientation effects depends strongly on the forest type/structure and the operation frequency. Regarding the influence of frequency, orientation effects are expected, in general, to be stronger at lower (e.g. P-band) than at higher frequencies (e.g. X-, or C-band). At L-band - an intermediate frequency band - the presence and intensity of orientation effects may vary from case to case depending on forest structure.

The Scots Pine forest stand simulation indicates the presence of significant orientation effects at L-band with differential extinctions on the order of 5-10 dB/m. However, the accuracy of those differential extinction estimates is questionable the modelling of vegetation extinction is in general affected by large error-bars. In contrary to these results, the analysis of several experimental Pol-InSAR data sets at L-band over temperate and boreal forest types (predominantly Pine, Spruce and/or Beach stands) do not indicate the presence of strong orientation effects – at least not as strong to effect the forest height estimation accuracy.

The lack of vegetation (forest and agriculture) extinction measurements and its variation with polarisation in the literature, for almost all key radar frequencies (X-, C-, and L-band) makes a critical evaluation of the obtained results very difficult. Thus, the organisation and support of experimental vegetation extinction/ attenuation measurement campaigns, especially with respect to future Pol-InSAR missions, is strongly recommended. In addition, acquisition and evaluation - with respect to forest height estimation and quantification of the effect of differential extinction - of experimental Pol-InSAR data over forest types characterised by different structure than the ones reported in the literature is also suggested. This will allow a wider validation of the proposed methodology and of the underlying assumptions.

In the absence of a ground elevation model the accuracy of the underlying phase estimation – and consequently the accuracy of the forest height estimation - depends critical on the choice of the polarisation pair. The performed analysis indicated that HH-VV and HV is the pair that leads to the best estimation performance. Under the constraint of a single transmission channel, HH and HV appears to provide the best results having at the same time the highest robustness against orientation effects. Light-Pol using circular polarisation LL and LR also provided satisfactory performance, at least in the simulated data sets used in this study. However, the fact that the circular performance is no better than the one obtained from the linear configuration combined with the fact that there are no plans for a near future makes the circular LL and LR pair to be of secondary importance.

IV.4 Quad-Pol and Temporal Decorrelation

Compared now to the Quad-Pol InSAR case, the main impairment regarding forest height estimation introduced by a Light-Pol InSAR configuration is in terms of robustness and estimation accuracy. A Quad-Pol InSAR configuration allows, as already mentioned above, a more accurate and/or robust estimation of the underlying topography phase as it allows to generate more statistical samples - in terms of linear combinations of the three independent polarisation states - required for a better

estimation. In the Light-Pol InSAR case, the availability of only two polarisations - that in both proposed configurations (HH and VH or LL and LR) do not correlate - affects the formation of appropriate linear combinations and limits thus the estimation accuracy/robustness.

In addition, a Quad-Pol InSAR configuration permits a more accurate approximation of the assumption of no ground scattering in one polarisation that is required for the regularisation of the inversion problem, especially in the presence of terrain variation. The availability of Quad-Pol data allows a better compensation of terrain induced ground scattering components, while in the Light-Pol InSAR case the assumption of no ground scattering is always approximated by the Cross-Pol channel. An external ground topography DEM becomes also on here of importance as it may permit the removal of the ground scattering components introduced by the terrain variation. The accuracy requirements are in this case not so strict as for the estimation of the phase related to the ground.

However, the main limitation for the application of the developed methodology is temporal decorrelation - inherent in all repeat-pass implementations of InSAR. Temporal decorrelation reduces the InSAR coherence and leads - if not accounted - to a sensitive overestimation of forest height. In its most general form, temporal decorrelation can affect directly the underlying *RVoG* inversion model making forest height estimation with a Light-Pol (or even Quad-Pol) InSAR configuration unreliable. However, the most common temporal decorrelation sources- as for example wind induced movement of the scatterers within the canopy layer - do not affect directly the underlying model, making forest height estimation a solvable but underdetermined problem at least for a for a single baseline Pol-InSAR acquisition. The most promising way to deal with this problem is by facing moderate decorrelation effects – guaranteed by very small temporal baselines – with an extended observation vector in terms of multiple interferometric observations at different baselines – a scenario that can be realised in the frame of a mission. In this way height retrieval with a reasonable error bar can be made possible (even for Light-Pol systems). Promotion for the development of the related methodology and its validation is highly recommended as a possible break-through will allow a significant upgrade of near future spaceborne SAR mission applications.

V DATA PROCESSING

(by DLR-IMF)

V.1 Snow and ice

DLR-IMF contributed to the retrieval of the snow water equivalent (SWE). The team processed interferometric data for the alpine test sites. For this task the interferometric processing system *GENESIS* which has proven its quality in ERS and SRTM processing was used. The delivered data sets include the differential interferogram, the coherence, the intensity image and the snow station locations mapped into the radar scene. These products were used complementary to the InSAR products produced by the ENVEO processing line, in order to reduce possible impacts of processing artefacts. In order to compensate the topography in the interferograms,

digital elevation models (DEM) from DLRs DEM data base were used. The best available DEM data was from the Shuttle Radar Topography Mission (SRTM).

The processing of the test site revealed some difficulties. Caused by the steep mountains and the low coherence the conventional coregistration based on correlation of image chips showed deficiencies. Therefore, a new and more robust coregistration algorithm was developed. The correlation of image chips was removed from the processing chain because of the strong influence of the temporal decorrelation on the resampling polynomial estimation. It was replaced by an algorithm that simulates the observation geometry using the scenes' orbits and a DEM reducing the number of unknown transformation parameters to two. The residual parameters, orbit and instrument timing offsets are corrected utilizing long time stable point scatterers. This automatically determined tie point information is merged with the geometrically computed resampling polynomial. All in all 66 interferograms were processed, quality inspected and delivered to ENVEO.

V.2 Atmosphere

Repeat pass InSAR observations are affected by atmospheric water vapour. This contribution is usually considered as an error in interferometry. In the recent years, techniques are developed which enable the separation of the different phase contributions, e.g. the Permanent Scatterer technique invented by POLIMI researchers. Water vapour especially affects the speed of the radar wave and can therefore be monitored as a geophysical variable applying the separation techniques.

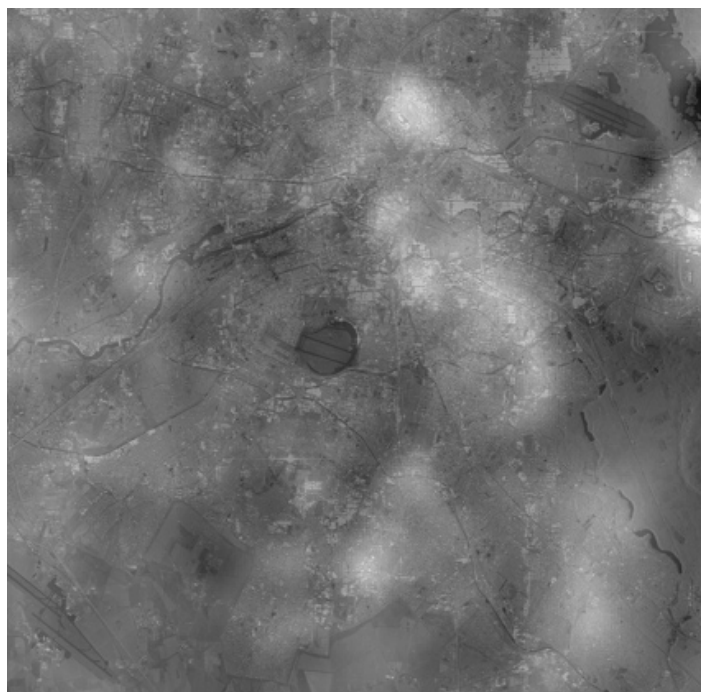


Figure V.1: Example for an atmospheric phase screen (APS) of a single scene utilising the Permanent Scatterer technique from the Berlin test site.

DLR-IMF supported the research by processing the interferometric data for two test sites. Two different processing techniques were applied. The Berlin data set is processed with the Permanent Scatterer technique using only selected points with coherence over long time. Figure V.1 shows the extracted atmospheric phase screen of a single scene. In comparison, a conventional cascaded differential interferometry processing was performed for the Las Vegas data. This was possible because of the long time coherence of the surrounding deserts.

The extracted atmosphere data were analysed by the researchers of the TU Delft. They assessed the properties of the atmosphere data. Caused by some unexpected results concerning the fractal property indicated by the power spectrum more detailed analyses were carried out by the DLR team. Firstly, the influence of the irregular sampling on the estimation of the fractal dimension was investigated. And secondly, the influence of noise on the fractal dimension estimation was checked. We found the fractal estimation very stable regarding the data sampling but noticed a strong influence of the noise power added to the fractal signals. Consequently, the noise budget in the Permanent Scatterer technique was examined in detail and reported. The presented theory is conform with the properties of the processed and delivered atmosphere data.

V.3 Conclusion and recommendations

It was advantageous to separate the data processing and the assessment of the data and to share the experience of the multi-disciplinary team. The use of SRTM DEMs to compensate the topographic phase contribution was very successful for the highly coherent Las Vegas data set even if the topography is very rough there. For the SWE estimation it seemed that interactively optimised standard double-differencing techniques showed slightly better results than the fully automatic processing using SRTM DEMs. The combined phase error contribution of the instrument and of temporal decorrelation to both applications should be studied in more detail in order to support operational services in the future.

VI REFERENCES

- [1] Guneriussen T., Høgda K.A., Johnson H. and Lauknes I. 2001. InSAR for estimating changes in snow water equivalent of dry snow, *IEEE Trans. Geosc. Rem. Sens.*, Vol. 39(10), 2101-2108.
- [2] Hanssen, R.F., A.J. Feijt, and R. Klees. 2001. Comparison of precipitable water vapor observations by spaceborne radar interferometry and Meteosat 6.7- μm radiometry. *J. of Atmosph. and Oceanic Techn.*, 18(5):756-764.
- [3] Hanssen, R.F., T.M. Weckwerth, H.A.Zebker, and R. Klees. 1999. High-resolution water vapor mapping from interferometric radar measurements. *Science*, 283:1295-1297, February 26.
- [4] Mätzler C., Microwave permittivity of dry snow. 1995. *IEEE Trans. Geosc. Remote Sensing*, Vol. 34(2), 573-581.

- [5] Misra A. and R. Scheiber, 2003. Differential Interferometric SAR Processing of E-SAR Data, *International Radar Symposium of India*, paper no. 121, pp. 624-633, Banalore, Dec. 2003.
- [6] Zebker H.A. and Villasenor J. 1992. Decorrelation in Interferometric Radar Echos. *IEEE Trans. Geosc. Rem. Sens.*, Vol. 30(5), 950-959.
- [7] Zebker H.A., P.A.Rosen, and S. Hensley. 1997. Atmospheric effects in interferometric synthetic aperture radar surface deformation and topographic maps, *J. of Geophys. Res.*, Vol. 102(B4), 7547-7563.



Innsbruck, AUSTRIA

Email: office@enveo.at

WWW: <http://www.enveo.at>